Upper Limb Deweighting using Underactuated End-effector based Backdrivable Manipulanda

V Crocher[1], J Fong[1], T Bosch[1,2], Y Tan[1], I Mareels[1], D Oetomo[1]

***Abstract*— In the rehabilitation for neurological injuries, gravity compensation or deweighting of the upper limb is often required as it allows patients with limited muscle activities to realise movements. Deweighting cancels the gravity effect of the human arm allowing the available muscle forces to produce acceleration, thus movements of the arm. This can be done through several approaches, such as joint-based approach (e.g. exoskeletons) and end-effector based (manipulanda), where the robot connects to the human arm at one point (usually the wrist or along the forearm) via its end-effector. Gravity compensation, in spatial (3D) cases, is done by applying the required forces at the end-effector of the robot.**

This paper formulates the gravity compensation strategy for spatial manipulanda, considers the effect of the force applied by the robotic device on the generalised dynamics of the upper limb and critically evaluates the advantages and limitations of this approach. Additionally, the proposed strategy is validated on the EMU robot, designed with the emphasis on its dynamic transparent mechanical transmission to allow impedance control approach. The EMU robot only has 3 degrees of actuation, making it underactuated with respect to the task of regulating a human arm up to the wrist modelled with 4 degrees of freedom. The underactuation resulted in an uncompensated gravity induced moment about the *swivel angle axis*, which is a line connecting the shoulder and wrist points of the human arm. The experimental validation demonstrates the effectiveness of the proposed gravity compensation technique in cancelling the effect of gravity on the user's arm.

I. INTRODUCTION

Robotic devices for neurological rehabilitation have been demonstrated to have a positive impact on the capabilities of patients, with many developed over the past two decades [1]. The capability of these robotic devices to provide engaging exercises with physical assistance, while minimising the requirement for physical therapist support speaks well to the goals of neurorehabilitation exercises, allowing a patient to perform many repetitions of goal-orientated movements (*i.e.* achieving a high dosage of treatment) [2], whilst being actively engaged.

A common practice in the rehabilitation of neurologically impaired patients is to 'deweight the arm' in clinical terms, or compensate for the gravity, in robotics terms. When a patient's arm is deweighted, it lowers the needed torque generated by the arm muscles to overcome the weight of the arm (to overcome the gravity component of the equation of motion of the patient's upper limb). When the gravity effect on the patient arm is completely compensated, then any muscle activities the patient possesses can be utilised to produce acceleration (thus movement) of the arm [3]. This is important as recovery from a neurological injury requires mass repetition of movements with patient involvement. Furthermore, this allows the patient to self initiate, achieve and observe more significant movement with their limited muscle activities. This provides a positive feedback loop towards exciting the brain-plasticity and regaining the motor function, as well as providing motivation. Deweighting is traditionally provided manually by the therapist supporting the weight of the patient arm, however, this manual manipulation is time consuming, physically exhausting and has been known to cause injury [4].

This work focuses on the deweighting capabilities of robot-assisted systems for the gross movements of the upper-limb. Conventionally, this can be generally categorised as one of two types: exoskeletons (joint based approach) and manipulanda (end-effector based approach). Exoskeleton robots aim to have an individual robotic joint for each physiological (human) joint, and thus have the advantages of arm support and motion regulation for all joints of the human arm — for example, the ARMin [5]. The downside is the potential joint misalignment (from the human joint) which can cause undesired forces to be applied to the patient [6]. Readjusting link lengths to match the joint kinematics of each patient also means an overhead in the clinical set up time. The design of exoskeletons, in particular the balancing the desired dynamics transparency and the effective (moving) inertia of the mechanism, is also a technically challenging problem [7].

Manipulanda, or end-effector based manipulators, do not suffer from many of the challenges faced by the exoskeletons mentioned above. However, manipulanda lose the joint specific control they can exert over the subject's upper-limb, thus requiring an end-effector based approach to be formulated. The challenge in balancing the dynamics transparency and the available end-effector forces, remains significant, resulting in mostly planar (2D) manipulanda being designed and used to this day, such as the MIT Manus [8]. This planar constraint means that many designs operate in this reduced workspace, which limits their applicability to moderately impaired patients and for more complex exercises; whereas many daily activities involve three dimensional (3D) movements. These limitations can be addressed through the development of 3D manipulanda such as the EMU [9] or the HapticMaster [10].

In the field of robotics, both categories of aforementioned devices, exoskeletons and manipulanda, can provide gravity compensation, whilst simultaneously providing additional as-

[1] Melbourne School of Engineering, University of Melbourne corresponding email: fong.j@unimelb.edu.au

[2] Eindhoven University of Technology (TU/e)

*This work is supported by the ARC Discovery Project DP160104018.

sistance, resistance or correction. Planar manipulanda, being restricted to a horizontal plane, perform gravity compensation by design, but are unable to provide partial deweighting. Exoskeletons provide the deweighting for each joint (*i.e.* upper-arm, forearm and hand) and compute compensation torques joint-by-joint (*i.e.* shoulder, elbow, wrist) [11]—operating under the assumption that their robotic structure aligns perfectly with the human limb kinematics.

Gravity compensation is not straightforward for a 3D manipulandum [9]. The required end-effector forces that needs to be applied to the human arm varies with the pose of the human arm. In [9], a preliminary simplified solution to this problem was proposed with an assumption of a rigid elbow joint angle.

In this paper, a gravity compensation algorithm for spatial manipulanda is proposed and comprehensively analysed. The method utilises the dynamics model of the human arm to provide a supporting force at the end-effector equivalent to the gravity component acting on the human arm strapped to the end-effector of the robot. The problem is formulated as one of finding the equivalent end-effector force that would result in zero torque on every joint of the human arm to maintain the current posture (statically). As such, the approach provides a quasi-static condition that suspends the patient's arm in its current pose, thus aiming to provide an equivalent gravity compensation effect of the support provided by exoskeletons.

The proposed algorithm is implemented on an underactuated manipulandum (EMU) [9] as an illustrative example and validation of its effectiveness in compensating the gravity forces on a mechanical arm.

The remainder of this paper is structured as follows. Section II proposes a mathematical description of the 'deweighting' problem for 3D manipulanda. Section III describes the proposed solution for the cases where the robotic manipulandum is fully actuated and underactuated. An experimental validation based on a mechanical representation of an arm are then presented in Section IV. Finally, the implications to the rehabilitation application are discussed in Section V.

II. PROBLEM DEFINITION

The overall system of interest can be defined as consisting of two components (see Figure 1): (1) the robotic device providing the deweighting force, described as kinematic chain r, and (2) the human upper-limb, described as kinematic chain h, whose weight and dynamics are to be compensated for. The two components are connected by having the human arm strapped onto the end-effector of the robotic device.

A. Robotic Device

The end-effector based manipulator considered in this paper is characterised by the feature that it is attached to the human arm at only a single location (at the forearm, see Figure 1) and allows movements in three dimensional space. It is also assumed that the forces $\mathbf{f}_r$ and moments $\mathbf{m}_r$ (*i.e.* wrench) applied to the human arm can be regulated by the robotic control strategy either through impedance or admittance control. In the case where the forces and moments in all directions can be applied, these would possess the dimensions of $\mathbf{f}_r \in \mathbb{R}^3$ and $\mathbf{m}_r \in \mathbb{R}^3$, however, it is not assumed that all devices under consideration have this property.

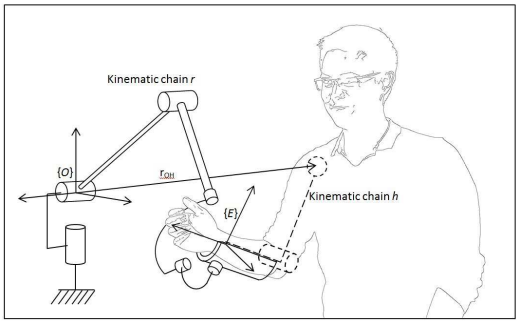

Fig. 1. The combined robot + human system using a manipulandum robot

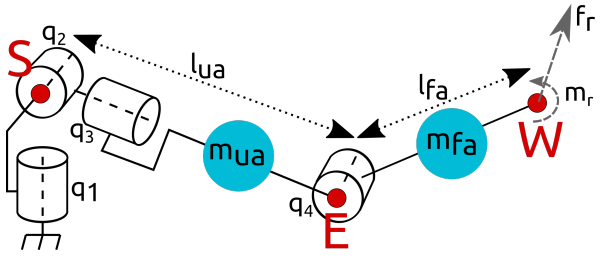

Fig. 2. The model of the human arm — a two links mechanism with 3 intersecting revolute joints q_1, q_2 and q_3 at the shoulder (S) and a revolute joint at the elbow E. W denotes the wrist location (*i.e.* contact location of the robotic device). Upper and lower arm are approximated by two links of lengths l_{ua} and l_{fas} and masses m_{ua} and m_{fa} respectively. $\mathbf{f}_r$ and $\mathbf{m}_r$ indicates the force and moment applied by the robotic manipulator.

B. Arm Model

The human arm is modelled as a 4DoFs two links serial mechanism. It consists of a shoulder joint (3DoFs), which is modelled as a spherical joint (3 revolute joints with intersecting axes) and a revolute elbow joint (1DoF). Mathematically, the joints are modelled as per the International Society of Biomechanical (ISB) recommendations [12], which is represented in Figures 2. The two rigid links therefore consist of the upper-arm and forearm with associated masses m_{ua} and m_{fa}, respectively, as depicted on Figure 2. It is assumed that the location of the shoulder is known in inertial space, allowing for a quasi static update of its location. The wrist joint is not considered, as the manipulandum is assumed to be connected to the end of the forearm of the subject. The displacements of the upper-limb joints are assumed to be known, which can be realised through direct measurements from external sensors (*e.g.* [13]) or from the kinematics of the robotic manipulandum if enough spatial information of the robot end-effector and / or displacement of the shoulder joint are known.

Whilst this model does not give a representation of all degrees of freedom in a human upper-limb, it models the degrees of freedom with the greatest ranges of motion in the

upper limb, and thus provides a suitable model for this work.

Given this model, the equations of motion of the human arm can be written as:

$$M_h(\mathbf{q}_h)\ddot{\mathbf{q}}_h + C_h(\mathbf{q}_h, \dot{\mathbf{q}}_h)\dot{\mathbf{q}}_h + \mathbf{g}_h(\mathbf{q}_h) = \boldsymbol{\tau}_h \quad (1)$$

where $\mathbf{q}_h, \dot{\mathbf{q}}_h$ and $\ddot{\mathbf{q}}_h \in \mathbb{R}^n$ are the generalised coordinates of the human arm and their derivatives, and $\boldsymbol{\tau}_h \in \mathbb{R}^n$ is the joint torque generated by the human subject (through activation of their muscles), $M_h(\mathbf{q}_h) \in \mathbb{R}^{n\times n}$ is the inertia matrix, $C_h(\mathbf{q}_h, \dot{\mathbf{q}}_h) \in \mathbb{R}^{n\times b}$ is the Coriolis and centrifugal matrix, and $\mathbf{g}_h(\mathbf{q}_h)$ is a vector corresponding to the gravitational terms. In the model used within this work, $n = 4$. It is noted that these equations are described with a subscript h (to denote human) to distinguish these variables from those attributed to the robotic device.

C. The Objective of 'Deweighting'

The robotic manipulandum needs to apply an end-effector force ($\mathbf{f}_r$) and moment ($\mathbf{m}_r$) to the human arm at point W (at the wrist). This forms an external wrench added to the equation of motion of the human arm (1), such that:

$$M_h(\mathbf{q}_h)\ddot{\mathbf{q}}+C_h(\mathbf{q}_h, \dot{\mathbf{q}}_h)\dot{\mathbf{q}}+\mathbf{g}_h(\mathbf{q}_h) = \boldsymbol{\tau}_h+\mathbf{R}_r(\mathbf{f}_r, \mathbf{m}_r) \quad (2)$$

where $\mathbf{R}_r(\mathbf{f}_r, \mathbf{m}_r)$ describes the wrench applied by the robot end-effector on human arm projected in the joint space of the human arm.

The aim of the arm deweighting strategy is to solve for the wrench ($[\mathbf{f}_r, \mathbf{m}_r]^T$) that the robotic end-effector needs to apply to compensate for the gravity force $\mathbf{g}_h(\mathbf{q}_h)$ acting on the human arm; such that zero torque is required at the shoulder and elbow joints to maintain a given pose of the human arm (for a *complete deweighting*). By extension, *partial deweighting* can be realised by compensating only for a portion of the gravity forces acting on the human arm, resulting in some remaining torque required at the shoulder and elbow joints for the human arm to overcome the effect of gravity. It is noted that such a reduction in the required torque is akin to reducing the amount of muscle forces required to overcome the weight of one's arm.

Remark: Note that the wrench applied by the robotic end-effector on the human arm will be projected into two components: one that acts upon the degrees of freedom of the human arm (*i.e.* the joints) and another that results in the reaction forces in the skeletal structure of the arm. The latter does not play any part in producing any acceleration (or movement) in the human arm, thus does not directly affect the deweighting process, but does have consequences in the clinical application in terms of reaction and contact forces in the skeletal and joints, respectively.

III. DEWEIGHTING STRATEGY

Within this section, a deweighting strategy is presented for the general class of joint torque commanded 3D manipulanda, capable of producing a commanded end-effector wrench.

The end-effector of the robotic manipulandum is strapped onto the forearm of the human user, applying wrench $[\mathbf{f}_r, \mathbf{m}_r]^T$ to the forearm of the human user at — and about — the wrist point W of the human arm. To achieve deweighting, the robot manipulandum should produce an end-effector wrench that results in a human joint space torque $\mathbf{R}_r(\mathbf{f}_r, \mathbf{m}_r) = \mathbf{g}_h(\mathbf{q}_h)$.

Given $n = 4$ is the number of degrees of freedom of the human arm (model) up to the forearm as presented in Section IIB and m is the number of actuated end-effector degrees of freedom of the robotic manipulandum, the deweighting strategy can be discussed as follows.

A. For Full-ranked Jacobian Transpose of the Human Arm

The quasi-static relationship between the wrench at the end-effector (applied by the robotic end-effector) and the joint torque of the human arm is expressed as:

$$\boldsymbol{\tau}_h = J_h^T(\mathbf{q}_h) \begin{bmatrix} \mathbf{f}_r \\ \mathbf{m}_r \end{bmatrix} \quad (3)$$

with J_h the Jacobian of the human arm, $\begin{bmatrix} \mathbf{f}_r \\ \mathbf{m}_r \end{bmatrix} \in R^m$ and $\boldsymbol{\tau}_h \in R^n$, where in our case $n = 4$. This means that the robot end-effector needs to be able to produce forces and moments in at least 4 degrees of freedom at the end-effector. However, note that due to the fact that this is a manipulandum, not an exoskeleton, the generalised coordinates representing the degrees of freedom of the robot and its associated generalised forces, are generally not one to one aligned with the joints of the human arm. Therefore, while we need at least 4 active degrees of freedom, generally more than 4 active DoFs are in practice needed of the robotic device to produce a full ranked Jacobian transpose J_h^T (*i.e.* $m > n$).

The required end-effector wrench for the deweighting procedure can then be calculated from the model of the human arm (2) as:

$$\begin{bmatrix} \mathbf{f}_r \\ \mathbf{m}_r \end{bmatrix} = J_h^{T\#}(\mathbf{q}_h)\ \mathbf{g}_h(\mathbf{q}_h) \quad (4)$$

where $J_h^{T\#}(\mathbf{q}_h)$ is a generalised inverse of the J_h^T, with $J \in R^{n\times m}$ and $m > n$. A least-square based generalised inverse, such as the Moore-Penrose pseudo inverse, will select an end-effector wrench with minimised norm. This has the effect of selecting the wrench to favour the component projected onto the degrees of freedom of the human arm and minimising the component projected into reaction forces into the skeletal system. A different choice of the resulting wrench that produces a different set of reaction forces can be realised by the use of null space projection of the desired behaviour, which would not affect the deweighting task (however, that is outside of the scope of this paper).

This provides a generic methodology for providing deweighting with any end-effector based device with full actuation in both force and moment. In such a case, J_h^T is full rank at postures other than singularities. In the case of the 4DoFs human arm model used in this case, the singularities occur at the straight elbow configuration and when the wrist point W is located vertically above the shoulder point S, which are equivalent to the elbow and head singularities in

anthropomorphic manipulators [14] [15]. In the rehabilitation robotics applications for which the deweighting procedure in this paper is considered, these singular configurations are (and can be) generally avoided and excluded from considerations.

In the case of a full ranked J_h^T, the gravity component of $\mathbf{g}(\mathbf{q}_h)$ can therefore be entirely compensated for, resulting in a complete deweighting scenario. The same can also be said about other exercises requiring joint-based force/motion regulation (of the joints of the human arm) - that they can be implemented in such fashion through an end-effector based robotic manipulandum.

B. On Underactuated Robotic Devices

In the interest of simplifying the robotic mechanism used for upper limb rehabilitation, it is desired to consider the application of the deweighting strategy on underactuated robots with only 3 degrees of actuation, capable of actively regulating the translational degrees of freedom of the end-effector. The orientation degrees of freedom is realised through a passive (non-actuated) spherical joint placed at the end-effector, where the angular displacements are measured. Such strategies can be found in rehabilitation spatial manipulanda designs such as the EMU [9] or HapticMaster [10].

In this case, the J_h^T matrix considers only the translational force components of the end-effector of the robotic manipulandum (as the actuation), while there are 4 joints considered in the model of the human arm that need to be manipulated:

$$\boldsymbol{\tau}_h = J_h^T(\mathbf{q}_h)\ \mathbf{f}_r \tag{5}$$

where $\boldsymbol{\tau}_h \in R^4$ and $\mathbf{f}_r \in R^3$.

The end-effector force that the robot manipulandum has to produce to achieve deweighting is therefore:

$$\mathbf{f}_r = J_h^{\mathrm{T}\#}(\mathbf{q}_h)\ \mathbf{g}(\mathbf{q}_h) \tag{6}$$

The system under consideration is therefore underactuated — only forces can be applied by the robot end-effector, in three directions ($\mathbf{f}_r \in \mathbb{R}^3$), however, the arm is modelled having four joints ($\mathbf{q}_h \in \mathbb{R}^4$). Thus, not all components of the gravity vector $\mathbf{g}_h(\mathbf{q}_h)$ (in joint space) can be completely compensated for at all times. In this case, the least square based generalised inverse minimises the error $||J_h^{\mathrm{T}\#}(\mathbf{q}_h)\ \mathbf{g}(\mathbf{q}_h) - \mathbf{f}_r||$.

It can be observed that the force $\mathbf{f}_r$ required as calculated in (6) varies across the workspace with $\mathbf{q}_h$ in magnitude and direction. Note that the force required to compensate for gravity at the end-effector of the robotic manipulandum is not only vertical in its direction because the load is not a single rigid body but a chain of rigid bodies. A visualisation of this force can be seen in Figure 3, which plots the calculated force in a number of postures in the sagittal plane, and in the transverse (horizontal) plane. The force changes at each of these postures, with larger forces required with more elbow extension, and more shoulder elevation. However, it is noted that, the magnitude and direction does not change significantly with differences in the transverse plane, associated with shoulder angle of elevation.

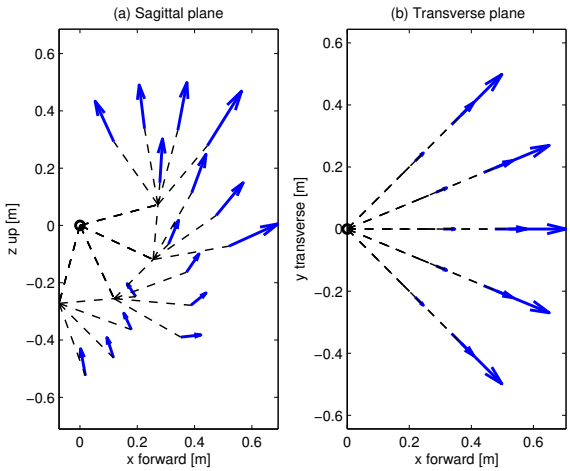

Fig. 3. Gravity compensation force for various arm postures in (a) Sagittal (vertical) plane and (b) Transverse (horizontal) plane. Black circle represents the shoulder position, dotted lines the arm posture.

The result of applying the proposed deweighting methodology to a manipulandum controlling only the force — and not the moments — at the end-effector can be identified by projecting the effects of the applied end-effector force back into the human joint space (*i.e.* the generalised coordinates):

$$\boldsymbol{\tau}_{comp} = J_h^{\mathrm{T}}(\mathbf{q}_h)\mathbf{f}_r \tag{7}$$

The component of the gravitational terms which are not compensated for by the deweighting algorithm can be expressed as:

$$\begin{aligned}\boldsymbol{\tau}_{uncomp} &= \mathbf{g}(\mathbf{q}_h) - J_h^{\mathrm{T}}(\mathbf{q}_h)\mathbf{f}_r &(8)\\ &= \mathbf{g}(\mathbf{q}_h) - J_h^{\mathrm{T}}(\mathbf{q}_h)J_h^{\mathrm{T}\#}(\mathbf{q}_h)\mathbf{g}(\mathbf{q}_h) &(9)\\ &= \left(I_4 - J_h^{\mathrm{T}}(\mathbf{q}_h)J_h^{\mathrm{T}\#}(\mathbf{q}_h)\right)\mathbf{g}(\mathbf{q}_h) &(10)\end{aligned}$$

with I_4 being the 4×4 identity matrix.

Based on Equation (10), these uncompensated moments lie in the null-space of J_h^T. They therefore do not affect any (linear) forces applied by the robot end-effector on the human arm. More specifically, as illustrated on Figure 4 the direction of the uncompensated moment is about an axis connecting the wrist point (W) and the shoulder joint (S) which is known as the *swivel angle axis*, defined and used for human-exoskeleton interaction analysis [16] and in rehabilitation applications [17]. It can therefore be seen that some shoulder torques are not compensated for whereas the elbow torque is fully compensated for in every posture, and that the magnitude of these torques is dependant on the posture.

IV. EXPERIMENTS

The proposed deweighting strategy, specifically for the underactuated case, is implemented on the EMU [9].

The EMU is a highly backdrivable system allowing for impedance control (see Figure 5) allowing 6DoFs movement of the end-effector, however, only the first 3 joints,

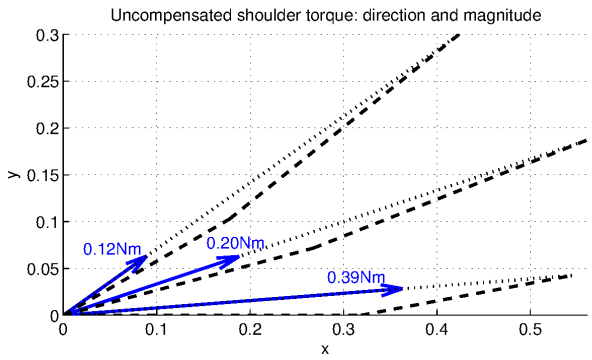

Fig. 4. The uncompensated moments (blue arrows) due to the use of an underactuated robot, are shown at the shoulder point (blue arrows) together with the swivel angle axis (dotted lines) for different arm postures (upper arm and forearm represented by dashed lines). Top View.

Fig. 5. The EMU backdrivable, end-effector based device for upper limb rehabilitation

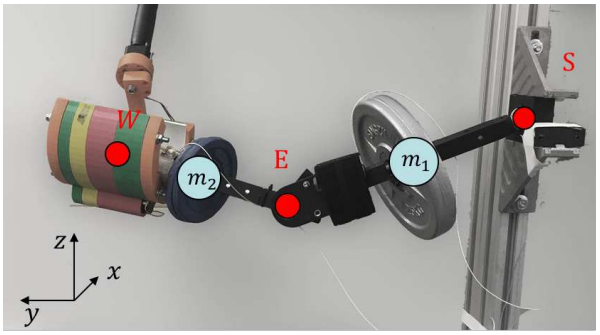

Fig. 6. The mechanical arm used in the experimental protocol. Locations representing the shoulder (S), elbow (E) and contact point (W) are labelled, as well as the two masses representing the mass of the arm.

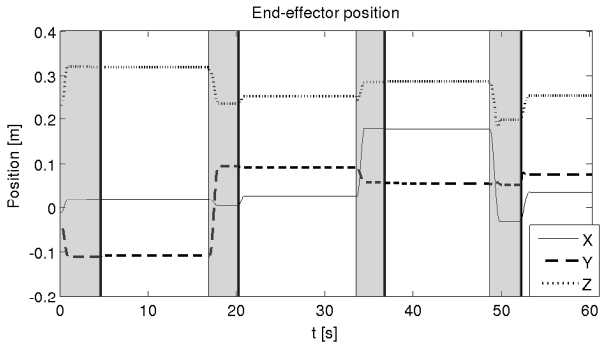

Fig. 7. Position of the end effector over time. Gray areas denote the position control periods to bring the end-effector to various positions, whereas clear areas denote the gravity compensation periods.

corresponding to the translation degrees of freedom of the robot end-effector are actuated. The displacements of the remaining DoFs, corresponding to the orientation of the end-effector, are measured but not actuated. The device is attached to the patient at the wrist end of the forearm.

A. Experiment Setup

A passive mechanical arm was constructed to serve as the load for the gravity compensation exercise representing a light human arm, as per the model identified in Figure 2, and can be seen in Figure 6. The mechanical arm consisted of two links connected to each other via a revolute joint, representing the elbow. One end was connected to a fixed frame via a spherical joint representing the shoulder, and the other end was connected to the end effector of the EMU manipulandum. Weights of $m_{ua} = 1kg$ and $m_{fa} = 1kg$ were secured respectively at the center of each link.

The mechanical arm is used for the experimental validation instead of a human subject because it is difficult to be sure that a human subject is truly "relaxed" at any given posture. The mechanical arm is fitted with high quality bearings at the elbow and shoulder joints to ensure that the joint torques are minimal, serving as a baseline study in worst case gravity compensation.

Magnetic sensors (trakSTAR, Ascension Technologies) were used to measure the orientation of the links, which was used to compute the posture of the mechanical arm $\mathbf{q}_h$ in real-time (at 60Hz). These were used in conjunction with an estimation of the model to calculate the required robotic force according to Equation (7).

B. Procedure

This described experiment setup was used to perform a validation experiment, demonstrate the feasibility of the deweighting control strategy and its possible implementation in real-time.

In this experiment, the robotic end-effector was moved by the robot to 4 different locations within the workspace in position control. These positions were chosen to cover the larger possible workspace allowed by the mechanical arm and thus assess the validity of the approach. Once each position was reached, the control was switched to the deweighting strategy. From this point, the response of the system was recorded.

C. Results

Figure 7 displays the end-effector position of the robot over time, *i.e.* the position of the contact point between the robotic device and the mechanical arm wrist point (W).

As can be observed, the system is capable of keeping stationary the mechanical arm at each posture that it was moved to. Some displacement error resulted, but generally settle quickly into a steady state. The displacement error from

TABLE I

ERROR DISTANCE FOR EACH POSTURE

Posture #	1	2	3	4
Error (mm)	2	31	2	87

the location where the controller is switched into deweighting algorithm is reported on Table I.

On the second and last postures, the robot and mechanical arm underwent a slightly noticeable displacement from the intended equilibrium position. It should be noted that the proposed strategy relies only on an open-loop compensation of the weight of the arm and thus the error can be explained by the difference between the identified the parameter dynamics values of the model and the actual mechanical arm as well as any postural measurements error. It should also be noted that compared to conventional robot with joint frictions and high gearing ratios, the EMU robot used here is highly backdrivable and very low in joint friction. Similarly, the mechanical arm used to represent the human arm in this experiment is also very low in joint friction. Thus the effect of mismatch easily manifests in visible motion. In a real rehabilitation application, a real human arm would provide plenty of damping and (muscle tone) stiffness, thus this error has not been observed to be significant.

V. DISCUSSION

The results presented in this paper provide a number of new insights regarding the use of three-dimensional end-effector based devices in the field of rehabilitation.

A. Other Devices and Clinical Application

Deweighting is commonly performed for rehabilitation of neurologically impaired patients. In lieu of devices, therapists often perform this manually, and passive devices exist which are designed to provide only deweighting support, such as the ArmeoSpring (Hocoma, Switzerland) and the SaeboMAS (Saebo, USA). Such devices can be mechanically tuned to provide different levels of support, but cannot impart or implement other control strategies.

Existing active robotic devices also provide deweighting functionality. 2D manipulanda provide deweighting by their planar design, however, cannot provide partial deweighting nor allow 3D exercises. Exoskeletons offer most flexibility in deweighting and control strategy, but can be difficult to set up and use in a clinical setting. The results within this work demonstrate that appropriately-designed end-effector based devices can provide deweighting support equivalent to that provided by an exoskeleton. An extension of these findings to other control strategies, such as discussed in [18], [19], [20], which have predominantly been implemented in exoskeleton-based robotic devices, may allow more advanced and effective strategies to be developed on simpler platforms — accelerating their translation to clinical practice.

However, concerns remain regarding the support of the device in other dimensions — for example, the analysis presented here only addresses the joint torques required at each location, and no consideration is given to interaction forces (through the assumption that the shoulder and elbow joints are ideal spherical and revolute joints, respectively). In reality, physiological joints are connected by ligaments and muscle, which do not always reflect the ideal representations — particularly with respect to stroke patients due to conditions such as subluxation. A further analysis may be constructed to estimate this, and to accommodate for this when deweighting.

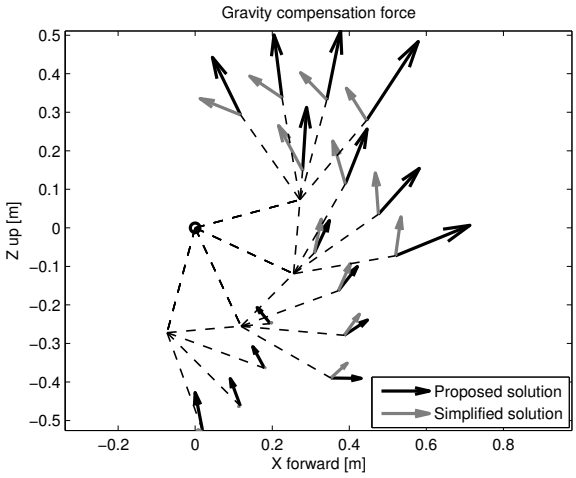

Fig. 8. Comparison between proposed deweighting control strategy, and simplified solution with rigid elbow joint presented in [9].

B. Existing Results

A previous 'simplified' deweighting control strategy was presented in [9]. In that previous work, the deweighting strategy implemented assumed a different model of the arm — that of a rigid elbow. As such, elbow torques were not compensated for. A comparison of the deweighting control algorithm detailed in the previous work, and the one proposed in this work can be seen in Figure 8.

It can be seen that there is a significant difference between the two, with the simplified solution proposing a force of smaller magnitude, which is always orthogonal to the vector between the shoulder and the contact location. It is thus expected that the use of the simplified solution may lead to error in the gravity compensation which may result in the patient's hand moving towards the shoulder (*i.e.* the elbow flexing). The proposed solution now includes a component of force of the same magnitude and in the same direction as the simplified solution, but also includes a orthogonal component which addresses the fact that the elbow is now considered as a joint. This 'pulls' the elbow joint outwards, such that it does not bend due to the effects of gravity.

C. Limitations and Practical Considerations

1) Requirement for Measurement: A limitation in the translation of this work to practice is the requirement that Jacobian $J_h(\mathbf{q}_h)$ and gravity vector $\mathbf{g}(\mathbf{q}_h)$ be known. This requires knowledge of the anthropomorphic characteristics of the patient arm and measurement of their posture in real time. However, it is noted that such knowledge is relatively robust to error and noise, due to the inherent

physical damping provided by having the human in the loop. Moreover it has been shown on exoskeleton devices that an anthropomorphic-based estimation is accurate enough for such application [11].

The measurement can be achieved through a variety of sensors — including sensors on the robotic device, magnetic sensors as used in this work, or Inertial Measurement Unit (IMU) sensors. In the specific case of the EMU, it is to note that only a measurement of the shoulder position would be required additionally to the measures of the system joints.

2) Uncompensated Torques: As discussed in Section III-B, in the case of an underactuated system, such as the EMU, some gravity torques are not compensated for. Nevertheless these torques being about the swivel angle are seen to be of minor importance as they do not contribute to any linear acceleration of the contact point and thus of the patient's hand. Moreover, the ability to completely compensate for the elbow torques in this approach was seen to be appropriate for upper-limb rehabilitation applications where patients often exhibit limitations in elbow movements, often compensated by trunk movements and associated with shoulder over abduction [21].

As such, although devices which can only provide forces (and not moments) at the end-effector does not physically prevent the use of these compensatory movements, it is still important that it does not passively encourage them. Furthermore, such movement patterns can be actively discouraged using indirect strategies, such as the one proposed in [17]. It is noted that these indirect strategies of corrections are potentially superior — as physically preventing a movement does not prevent the muscle activation patterns. In fact, it suppresses its effects, which may be counter-productive to discouraging the activation patterns to start with.

VI. CONCLUSIONS

Within this work, a gravity compensation strategy for deweighting a patient's arm with three dimensional end-effector based devices has been proposed. Specific study was carried out on the strategy using a 4 degree of freedom arm model, where the robotic device is underactuated with respect to the task, due to its inability to provide moments at the end-effector. Such an arrangement was found to negate the effects of gravity, except for moments about the axis connecting the shoulder and contact location point (the swivel angle axis).

Further experimental works are necessary to evaluate the effect and reaction of the proposed strategy with both healthy subjects and neurologically impaired patients. Considerations of the effect of the applied forces on the reaction forces on the joints need to be studied in the clinical context.

REFERENCES

[1] P Maciejasz, J Eschweiler, K Gerlach-Hahn, A Jansen-Troy, and S Leonhardt. A survey on robotic devices for upper limb rehabilitation. *Journal of Neuroengineering and Rehabilitation*, 11(1):3, 2014.

[2] VS Huang and JW Krakauer. Robotic neurorehabilitation: a computational motor learning perspective. *Journal of Neuroengineering and Rehabilitation*, 6(1):5, 2009.

[3] MJA Jannink, Grada Berendina Prange, AHA Stienen, Herman van der Kooij, JM Kruitbosch, Maarten Joost IJzerman, and Hermanus J Hermens. Reduction of muscle activity during repeated reach and retrieval with gravity compensation in stroke patients. In *IEEE Int'l Conf Rehab Rob (ICORR)*, pages 472–476. IEEE, 2007.

[4] SP Anderson and J Oakman. Allied health professionals and work-related musculoskeletal disorders: A systematic review. *Safety and Health at Work*, 7(4):259–267, 2016.

[5] T Nef, M Mihelj, G Colombo, and R Riener. ARMin-robot for rehabilitation of the upper extremities. In *Proceedings 2006 IEEE International Conference on Robotics and Automation (ICRA 2006)*, pages 3152–3157. IEEE, 2006.

[6] N Jarrasse and G Morel. Connecting a human limb to an exoskeleton. *IEEE Transactions on Robotics*, 28(3):697–709, 2012.

[7] J Fong, V Crocher, D Oetomo, Y Tan, and I Mareels. Effects of robotic exoskeleton dynamics on joint recruitment in a neurorehabilitation context. In *14th IEEE/RAS-EMBS International Conference on Rehabilitation Robotics*, pages 834–839, 2015.

[8] N Hogan, HI Krebs, J Charnnarong, P Srikrishna, and A Sharon. MIT-MANUS: a workstation for manual therapy and training. i. In *Proceedings of 1992 IEEE International Workshop on Robot and Human Communication*, pages 161–165. IEEE, 1992.

[9] J Fong, V Crocher, Y Tan, D Oetomo, and I Mareels. EMU: a transparent 3d robotic manipulandum for upper-limb rehabilitation. In *IEEE Int'l Conf Rehab Rob (ICORR)*, pages 771–776. IEEE, 2017.

[10] MJ Johnson, KJ Wisneski, J Anderson, D Nathan, and RO Smith. Development of ADLER: the activities of daily living exercise robot. In *IEEE/RAS-EMBS Int'l Conf Biomed Rob & Biomechatr (BioRob 2006)*, pages 881–886, 2006.

[11] F Just, Ö Özen, S Tortora, R Riener, and G Rauter. Feedforward model based arm weight compensation with the rehabilitation robot armin. In *IEEE Int'l Conf Rehab Robot (ICORR)*, pages 72–77, 2017.

[12] G Wu, FCT Van der Helm, HEJDJ Veeger, M Makhsous, P Van Roy, C Anglin, J Nagels, AR Karduna, K McQuade, X Wang, et al. ISB recommendation on definitions of joint coordinate systems of various joints for the reporting of human joint motionpart ii: Shoulder, elbow, wrist and hand. *Journal of Biomechanics*, 38(5):981–992, 2005.

[13] M van Lith, J Fong, V Crocher, Y Tan, D Oetomo, and I Mareels. Calibration free upper limb joint motion estimation algorithm with wearable sensors. In *Procs. International Conference Control, Automation, Robotics and Vision (ICARCV2016)*, 2016.

[14] D Oetomo and MH Jr. Ang. Singularity robust algorithm in serial manipulators. *Robotics and Computer-Integrated Manufacturing*, 25(1):122–34, 2009.

[15] D Oetomo, MH Jr Ang, and SY Lim. Singularity handling on puma in operational space formulation. In *Lecture Notes in Control and Information Sciences*, volume 271, pages 491–501, 2001.

[16] H Kim, LM Miller, A Al-Refai, M Brand, and J Rosen. Redundancy resolution of a human arm for controlling a seven dof wearable robotic system. In *Int'l Conf Eng Med & Biol Soc*, pages 3471–3474, 2011.

[17] EB Brokaw, PS Lum, RA Cooper, and BR Brewer. Using the kinect to limit abnormal kinematics and compensation strategies during therapy with end effector robots. In *IEEE Int'l Conf Rehab Rob (ICORR)*, pages 1–6. IEEE, June 2013.

[18] SH Zhou, J Fong, V Crocher, Y Tan, D Oetomo, and I Mareels. Learning control in robot-assisted rehabilitation of motor skills–a review. *Journal of Control and Decision*, 3(1):19–43, 2016.

[19] A Basteris, SM Nijenhuis, AHA Stienen, JH Buurke, GB Prange, and F Amirabdollahian. Training modalities in robot-mediated upper limb rehabilitation in stroke: a framework for classification based on a systematic review. *Journal of Neuroengineering and Rehabilitation*, 11(1):111, 2014.

[20] AU Pehlivan, DP Losey, and MK O'Malley. Minimal assist-as-needed controller for upper limb robotic rehabilitation. *IEEE Transactions on Robotics*, 32(1):113–124, 2016.

[21] MF Levin. Interjoint coordination during pointing movements is disrupted in spastic hemiparesis. *Brain*, 119(1):281–293, 1996.